Zero Voltage Vector Based Initial Magnet Polarity Identification Strategy of PMSM Drives

Kairan Wang[1], Guoqiang Zhang [1], Rundong Li[1],Yang Hua[1], Gaolin Wang[1], and Dianguo Xu[1]
[1] Harbin Institute of Technology, China

***Abstract*-- Accurate identification of magnet polarity seriously affects the accuracy of the initial position of a permanent magnet synchronous motor (PMSM) drive during flying start. In this paper, a novel magnet polarity identification method based on zero voltage vector (ZVV) pulse is proposed for flying start. According to the relationship between the current vector position and the initial position observed through high frequency signal injection method, an initial magnet polarity identification with high fault tolerance performance is proposed to improve the region misclassification problem which is caused by current sampling errors. The proposed method could accurately identify the magnet position at low speeds and improve the reliability of the initial position identification at flying start. The proposed method is validated on a 2.2-kW PMSM drive.**

***Index Terms*--Permanent magnet synchronous motor, flying start, initial magnet polarity identification, zero voltage vector**

I. INTRODUCTION

Permanent magnet synchronous motor (PMSM) is widely used in the industrial production because of its high efficiency and high-power density [1]. Sensorless control provides the advantage of low cost and high reliability by collecting current or voltage for position observation [2]. However, for some specific applications such as air conditioning fans, the rotor may rotate slowly before starting. Therefore, it is necessary to observe the initial position and then apply the observation results to sensorless control so as to realize the flying start [3].

A lot of research has been done on the initial position recognition of the rotating state of the motor. In [4], a zero-voltage vector pulse method based on the initial position recognition algorithm in the rotating state is proposed, but the algorithm is only suitable for initial position recognition at medium and high speeds, and requires multiple pulse injections, making the observation convergence slow. In [5], an algorithm for initial position identification based on the concept of virtual resistance is proposed, which is used to control the band speed rethrow current by adjusting the virtual resistance introduced in the αβ coordinate system, and then to simulate the three-phase variable resistance with an inverter using the approximate purely resistive nature of the system equivalent circuit, adjusting this virtual resistance and observing the initial rotor position or speed according to the stator current. This method is suitable for a wide range of initial speeds, but the virtual resistance varies with the initial speed, resulting in inconsistent observation accuracy.

In order to achieve accurate position recognition at low speeds, a combined scheme of high frequency (HF) signal injection and magnet polarity identification has been introduced by scholars [5], the HF signal injection based method is widely used for position and speed observation because of high reliability and excellent dynamic performance [6]. However, the initial position observation using the HF signal injection based method may converge to the d-axis or the -d-axis. Therefore, it is necessary to carry out the magnet polarity identification after the initial position observation [7].

The available initial magnet polarity identification methods include double pulse method and d-axis current peak accumulation method [8]. The double pulse injection based magnet polarity identification method achieves initial magnet polarity identification based on the current response by injecting two consecutive voltage pulses in the d-axis and -d-axis [9]. The second pulse needs to be separated from the first pulse for a period of time. However, in the case of motor operation, the rotor may rotate by a certain angle during the interval, resulting in inaccurate injection of the second pulse. The magnet polarity identification method based on peak d-axis current accumulation is based on injecting a HF square-wave into the system, collecting and accumulating the current amplitude in each d-axis, and identifying the poles by the result of the accumulated current [5]. However, it takes a long time to collect the current accumulation, and the trend of the accumulation result is not obvious, and it may jump up and down around the zero point, which affects the speed and accuracy of magnet polarity identification [4].

In order to improve the flying start performance of the PMSM drives, this paper proposes a magnet polarity identification strategy using a ZVV single pulse. Faster and more accurate magnet polarity identification could be achieved by applying a short ZVV single pulse and exciting the current vector, and then combining the current vector position and the rotor position observed by the HF injection method. This magnet polarity identification strategy is highly reliable and fault tolerant. The proposed method is implemented on a 2.2-kW PMSM experimental platform, which verifies the effectiveness and accuracy.

II. THE PROPOSED MAGNET POLARITY IDENTIFICATION STRATEGY

A. Mathematical Model of PMSM

In the rotary reference frames, the stator voltage equation of PMSM is:

This work was supported in part by the Research Fund for the National Natural Science Foundation of China under Grants 52177034 and 52125701, and in part by the Fundamental Research Funds for the Central Universities under Grants FRFCU5710092020 and FRFCU5710051220.

$$\begin{bmatrix} v_{\mathrm{d}} \\ v_{\mathrm{q}} \end{bmatrix} = \begin{bmatrix} R_{\mathrm{s}} & -\omega L_{\mathrm{q}} \\ \omega L_{\mathrm{d}} & R_{\mathrm{s}} \end{bmatrix} \begin{bmatrix} i_{\mathrm{d}} \\ i_{\mathrm{q}} \end{bmatrix} + \begin{bmatrix} L_{\mathrm{d}} & 0 \\ 0 & L_{\mathrm{q}} \end{bmatrix} \frac{\mathrm{d}}{\mathrm{d}t} \begin{bmatrix} i_{\mathrm{d}} \\ i_{\mathrm{q}} \end{bmatrix} + \begin{bmatrix} 0 \\ \omega \psi_{\mathrm{f}} \end{bmatrix} \tag{1}$$

where u_{d}, u_{q}, i_{d}, i_{q} are the d- and q-axis voltages and currents respectively. ω_e is the electrical rotor speed. R_s is the stator resistance. p is the differential operation d/dt. ψ_f is the motor permanent magnet flux linkage, L_{d} and L_{q} denote the d-q axis inductances.

B. HF Signal Injection Based Rotor Position Identification

The initial position angle is observed at low speeds using the HF square wave voltage injection. The expression for the injected voltage signal is:

$$u_{\mathrm{inj}} = \begin{cases} U_{\mathrm{inj}}, t \in \left[nT_{\mathrm{inj}}, \left(n + \frac{1}{2} \right) T_{\mathrm{inj}} \right] \\ -U_{\mathrm{inj}}, t \in \left[\left(n + \frac{1}{2} \right) T_{\mathrm{inj}}, (n+1) T_{\mathrm{inj}} \right] \end{cases} \tag{2}$$

where U_{inj} is the amplitude of the injected voltage signal, T_{inj} is the injection period of the HF signal and n is the number of periods of the injected signal.

The reference frames used for the analysis of PMSM low speed sensorless control based on HF square wave voltage injection is illustrated in Fig. 1, where α-β , d-q , $\mathrm{d^e}$-$\mathrm{q^e}$ and $\mathrm{d^m}$-$\mathrm{q^m}$ axes represent the stationary, rotational, estimation and measurement frames respectively.

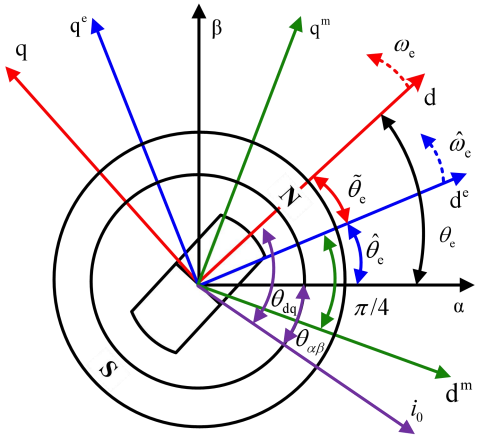

Fig. 1. Coordinate system of the PMSM drive.

At zero speed and low speed operating conditions, since the injection signal frequency is much higher than the motor running frequency, the rotor speed term included in can be ignored. At the same time, the inductive resistance of an inductor is usually much greater than the impedance of the stator winding resistance, so the voltage drop caused by the resistance can be ignored. The HF PMSM model can be expressed as：

$$\begin{bmatrix} u_{\mathrm{dh}} \\ u_{\mathrm{qh}} \end{bmatrix} = \begin{bmatrix} L_{\mathrm{dh}} & 0 \\ 0 & L_{\mathrm{qh}} \end{bmatrix} \mathrm{p} \begin{bmatrix} i_{\mathrm{dh}} \\ i_{\mathrm{qh}} \end{bmatrix} \tag{3}$$

where $u_{\mathrm{dh,qh}}$ and $i_{\mathrm{dh,qh}}$ are HF voltages and induced currents in rotor frame, respectively.

Also between the d-q framework and the $\mathrm{d^e}$-$\mathrm{q^e}$ framework there is the following relationship:

$$\begin{bmatrix} u_{\mathrm{dh}} \\ u_{\mathrm{qh}} \end{bmatrix} = T\left(\tilde{\theta}_{\mathrm{e}} \right) \begin{bmatrix} u_{\mathrm{dh}}^{\mathrm{e}} \\ u_{\mathrm{qh}}^{\mathrm{e}} \end{bmatrix} \tag{4}$$

Where u_{dh}^{e} and u_{qh}^{e} are the HF voltage components in the $\mathrm{d^e}$-$\mathrm{q^e}$ frame, respectively; $\tilde{\theta}_e$ is the error between the actual and observed positions; $T(\cdot)$ is the coordinate transformation matrix, which can be expressed as:

$$T(\cdot) = \begin{bmatrix} \cos(\cdot) & \sin(\cdot) \\ -\sin(\cdot) & \cos(\cdot) \end{bmatrix}. \tag{5}$$

The HF voltage is injected in the observation frame and the $\mathrm{d^e}$-$\mathrm{q^e}$ frame voltage equation is:

$$\begin{bmatrix} u_{\mathrm{dh}}^{\mathrm{e}} \\ u_{\mathrm{qh}}^{\mathrm{e}} \end{bmatrix} = \begin{bmatrix} u_{\mathrm{inj}} \\ 0 \end{bmatrix} = T^{-1}(\tilde{\theta}_{\mathrm{e}}) \begin{bmatrix} L_{\mathrm{dh}} & 0 \\ 0 & L_{\mathrm{qh}} \end{bmatrix} T(\tilde{\theta}_{\mathrm{e}}) \cdot \mathrm{p} \begin{bmatrix} i_{\mathrm{dh}}^{\mathrm{e}} \\ i_{\mathrm{qh}}^{\mathrm{e}} \end{bmatrix} \tag{6}$$

where i_{dh}^{e} and i_{qh}^{e} are the HF response current components in the $\mathrm{d^e}$-$\mathrm{q^e}$ frame, respectively.

From , the HF response current signal in the $\mathrm{d^e}$-$\mathrm{q^e}$ frame is obtained as:

$$\begin{bmatrix} \mathrm{p}i_{\mathrm{dh}}^{\mathrm{e}} \\ \mathrm{p}i_{\mathrm{qh}}^{\mathrm{e}} \end{bmatrix} = \frac{u_{\mathrm{inj}}}{L_{\mathrm{dh}} L_{\mathrm{qh}}} \begin{bmatrix} L_0 - L_1 \cos\left(2\tilde{\theta}_{\mathrm{e}} \right) \\ -L_1 \sin\left(2\tilde{\theta}_{\mathrm{e}} \right) \end{bmatrix}. \tag{7}$$

The HF response currents excited by HF square wave voltage signals contain rotor position information. The rotor position error signal can therefore be decoupled from the HF response current. The $\mathrm{d^e}$-$\mathrm{q^e}$ frame and the current in the $\mathrm{d^m}$-$\mathrm{q^m}$ frame satisfy the following relationship:

$$\begin{bmatrix} i_{\mathrm{dh}}^{\mathrm{m}} \\ i_{\mathrm{qh}}^{\mathrm{m}} \end{bmatrix} = T\left(-\frac{\pi}{4} \right) \begin{bmatrix} i_{\mathrm{dh}}^{\mathrm{e}} \\ i_{\mathrm{qh}}^{\mathrm{e}} \end{bmatrix} \tag{8}$$

where $i_{\mathrm{dh}}^{\mathrm{m}}$ and $i_{\mathrm{qh}}^{\mathrm{m}}$ separate the HF current signals for measuring shaft systems, respectively.

Fig. 2 shows the current response sequence diagram. Since the HF response current varies with time in a periodic triangular wave, the absolute value of the separated HF response current is processed. At the same time, the non-negative signal can be seen as a superposition of alternating positive and negative triangular wave signals and DC signals at the same frequency as the signal.

The DC signal is influenced by the amplitude of the HF response current, which contains rotor position information. So a low-pass filter can be used to separate out the DC component containing the rotor position tracking error, and thus obtain the HF current amplitude, as shown in:

$$\begin{bmatrix} I_{\mathrm{dh}}^{\mathrm{m}} \\ I_{\mathrm{qh}}^{\mathrm{m}} \end{bmatrix} = \frac{\sqrt{2}}{4} \frac{U_{\mathrm{inj}} T_{\mathrm{inj}}}{L_{\mathrm{dh}} L_{\mathrm{qh}}} \begin{bmatrix} L_0 - L_1 \cos\left(2\tilde{\theta}_{\mathrm{e}} \right) + L_1 \sin\left(2\tilde{\theta}_{\mathrm{e}} \right) \\ L_0 - L_1 \cos\left(2\tilde{\theta}_{\mathrm{e}} \right) - L_1 \sin\left(2\tilde{\theta}_{\mathrm{e}} \right) \end{bmatrix}. \tag{9}$$

The extracted HF current amplitude is standardization to obtain the equivalent position error signal ε:

$$\varepsilon = \frac{I_{\mathrm{dh}}^{\mathrm{m}} - I_{\mathrm{qh}}^{\mathrm{m}}}{\sqrt{(I_{\mathrm{dh}}^{\mathrm{m}})^2 + (I_{\mathrm{qh}}^{\mathrm{m}})^2}} \approx \frac{L_{\mathrm{dh}} - L_{\mathrm{qh}}}{\sqrt{2} L_{\mathrm{qh}}} \sin\left(2\tilde{\theta}_{\mathrm{e}} \right). \tag{10}$$

To improve the robustness of the observer input to the motor parameters and input voltage amplitude, the

extracted HF current amplitude is standardization to obtain the final equivalent position error signal ε. The PI-type phase-locked loop is used to converge the rotor position observation error to zero, which in turn gives the rotor position and speed information.

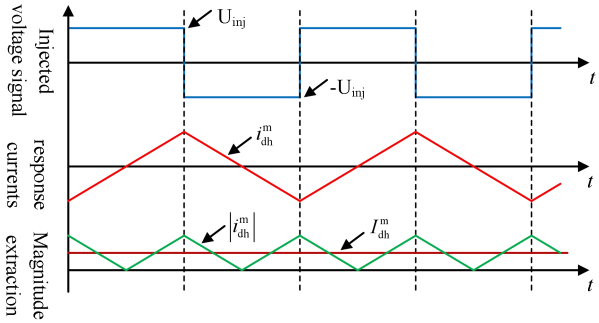

Fig. 2 Current Response Sequence Diagram

C. *Position of Current Vector Excited by ZVV Pulse*

When a ZVV pulse is applied, $v_d = v_q = 0$, the stator winding forms a path with the three switching tubes to produce a short-circuit current containing the initial position and speed information. The current vector $\boldsymbol{i_0} = [i_\alpha, i_\beta]$ is shown in Fig. 1. $\theta_{\alpha\beta}$, θ_{dq} and θ_e are the position of the current vector in the α-β frame, the d-q frame and the position of the rotor, respectively.

Since the stator current excited by the ZVV pulse is small, the stator resistance voltage drop can be ignored in the calculation process, and the voltage equation can be approximated as:

$$\begin{bmatrix}0\\0\end{bmatrix}=\begin{bmatrix}0 & -\omega L_q\\ \omega L_d & 0\end{bmatrix}\begin{bmatrix}i_d\\ i_q\end{bmatrix}+\begin{bmatrix}L_d & 0\\ 0 & L_q\end{bmatrix}\frac{d}{dt}\begin{bmatrix}i_d\\ i_q\end{bmatrix}+\begin{bmatrix}0\\ \omega\psi_f\end{bmatrix}. \quad (11)$$

The position of the current vector in the dq-axis can be obtained by solving:

$$\theta_{dq}=\tan^{-1}\left(i_q,\ i_d\right)=\begin{cases}-\dfrac{L_q}{2L_d}\omega T_c-90°, & \omega>0\\ -\dfrac{L_q}{2L_d}\omega T_c+90°, & \omega<0\end{cases}. \quad (12)$$

When the PMSM rotates forward, $\omega>0$, $i_d<0$, $i_q<0$, and $|i_q| >> |i_d|$. Therefore, the current vector is near q-axis and slightly lags behind the q-axis, as shown in Fig. 1. When the PMSM rotates backward, $\omega<0$, $i_d<0$, $i_q>0$ and $|i_q| >> |i_d|$. The current vector is near q-axis and slightly lags behind the q-axis. In addition, the position of current vector excited by the ZVV pulse has nothing to do with the actual position of PMSM. Therefore, this fixed relation can be used to identify initial magnet polarity.

III. ZVV Based Magnet Polarity Identification Method

The control block diagram of PMSM initial magnet polarity identification is shown in Fig. 3.

At flying start, the motor starts HF injection, the initial position converges and after applying ZVV pulse, the range of the current vector position can be obtained. Combining the initial position obtained by the HF signal injection method with the current vector position obtained by the ZVV method, the current magnet polarity can be determined by the correspondence between the two. In this paper, the range of the current vector is divided into four regions: (315°, 45°), (45°, 135°), (135°, 225°), (225°, 315°).

Fig. 4(a) and Fig. 4(b) shows the relationship between the current vector and the rotor position when PMSM rotates forward and reverse respectively. the current vector is in the range of (315°, 45°) in (I and II).

For example, when PMSM is rotating forward and the current vector is located in the range of (315°, 45°), the identification result of initial magnet polarity is magnetic

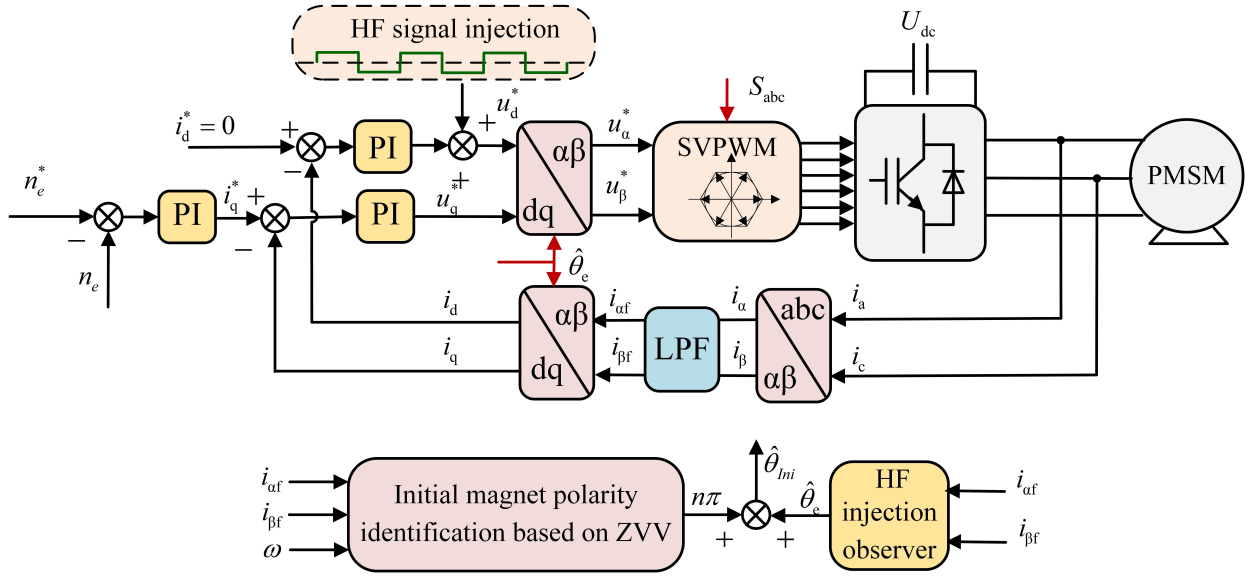

Fig. 3 The control block diagram of PMSM initial magnet polarity identification.

North (N) pole if the position measured by HF signal injection based method is located in the first or second quadrant. Instead, the identification result is magnetic South (S) pole. In the similar way, the initial magnet polarity can also be identified when the current vector is in other quadrants or the PMSM rotates backward.

The relationship between the current vector and the initial magnet polarity in the case of forward and reverse rotation, respectively, is shown in Table II, Table II.

When the current vector is located near $\theta_{\alpha\beta}=k*45°$, ($k$ =1,2), the values of i_α and i_β are similar, which easily leads to the error of region judgment. For example, in $\theta_{\alpha\beta}=40°$ may be misinterpreted as $\theta_{\alpha\beta}=50°$. In both cases, the actual position of d-axis is in the second quadrant, respectively within and outside the range of region III. When $\theta_{\alpha\beta}$ is misjudged as $\theta_{\alpha\beta}=50°$, the current vector belongs to the range (45°, 135°). According to Table I, when the current vector is in the range of (45°, 135°) and the rotor position in the range of second quadrant, it is still judged as d-axis, thus the initial magnet polarity identification result is magnetic N pole, which is consistent with the identification result in the case of no misjudgment. The same principle applies to reverse rotation or misjudgment of the current vector region at other angles. It can be found that this method has high fault-tolerance performance for regional misjudgment caused by current sampling error at the boundary of the region.

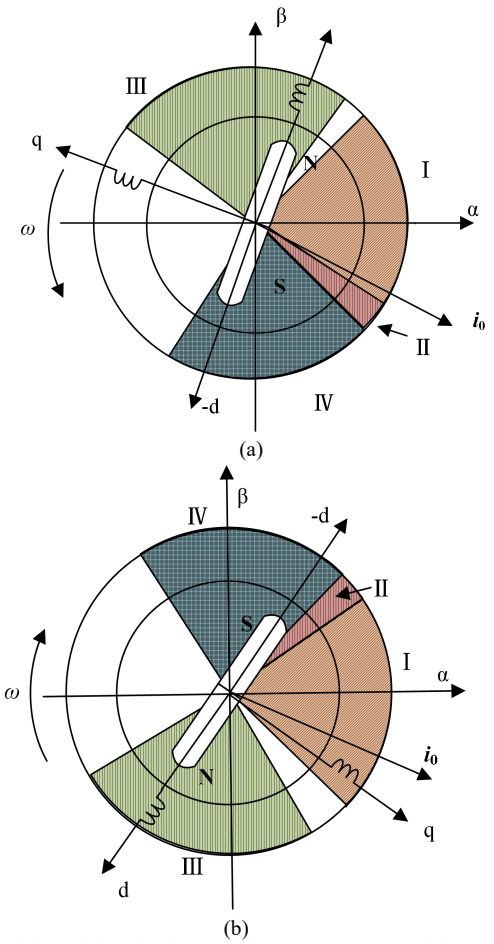

Fig. 4. Position relationship between the current vector and the magnetic poles.

TABLE I.
THE RELATIONSHIP BETWEEN THE CURRENT VECTOR AND THE INITIAL MAGNET POLARITY (ROTATES FORWARD)

current vector position	d-axis position	- d-axis position
(-45°, 45°)	1, 2	3, 4
(45°, 135°)	2, 3	4, 1
(135°, 225°)	3, 4	1, 2
(225°, 315°)	4, 1	2, 3

TABLE II.
THE RELATIONSHIP BETWEEN THE CURRENT VECTOR AND THE INITIAL MAGNET POLARITY (ROTATES REVERSE)

current vector position	d-axis position	- d-axis position
(-45°, 45°)	3、4	1、2
(45°, 135°)	4、1	2、3
(135°, 225°)	1、2	3、4
(225°, 315°)	2、3	4、1

The proposed initial magnet polarity identification strategy based on ZVV in this paper can calculate the range of the current vector through applying a short ZVV pulse, so as to realize the initial magnet polarity identification. More importantly, it can effectively overcome the sampling error of i_α and i_β and has high reliability.

IV. SIMULATION AND EXPERIMENTAL RESULTS

A. Simulation and Analysis

A simulation model was built for the simulation, setting the initial speed of the motor to 100r/min and then repeatedly applying a single pulse of ZVV at a fixed frequency and repeating the magnet polarity identification.

If the recognition result is N pole then 0° is compensated. Conversely, if the result is S pole, 180° is compensated and the compensated rotor position is output.

Fig. 5 show the results of the magnet polarity identification simulation for an initial speed of 100r/min, from top to bottom: the amplitude of the stator current vector excited by the ZVV pulse, the actual position of the rotor; the rotor position observed by HF injection and the rotor position after magnet polarity identification and the sampled value of the stator current in the α-β frame.

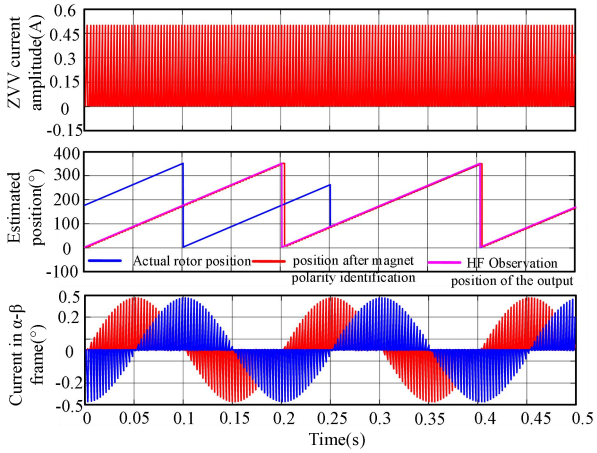

Fig. 5 Simulation results for magnet polarity identification

In the range of 0 to 0.25s, the rotor position observed by the HF injection method converges to the S pole, and in the range of 0.25 to 0.5s, the rotor position observed by the HF injection method converges to the N pole.

In the simulation, when the rotor position observed by the HF injection method converges to the S pole, 180° compensation is added to the original position to coincide with the actual initial position; in the interval of 0.25-0.5s, no compensation is required to complete the magnet polarity identification and the rotor position is identical to the actual position.

The simulation results show that, ideally, the current sampling is accurate, the quadrant range of the current vector is correct, the studied methods can effectively carry out magnet polarity identification, and the current vector amplitude excited by the zero voltage vector pulse is small, which has no effect on the normal operation of the motor.

B. Experimental Setup

The proposed scheme is validated on a 2.2-kW PMSM platform, as depicted in Fig. 6. Couplings connect the PMSM to the induction motor. The induction motor can be controlled to provide the initial speed or load torque for the PMSM, and the two inverters are connected by a common DC bus. The STM32F103VCT6 ARM control chip implements software algorithms to control the PMSM with a current sampling frequency of 10kHz in conjunction with the inverter switching frequency.

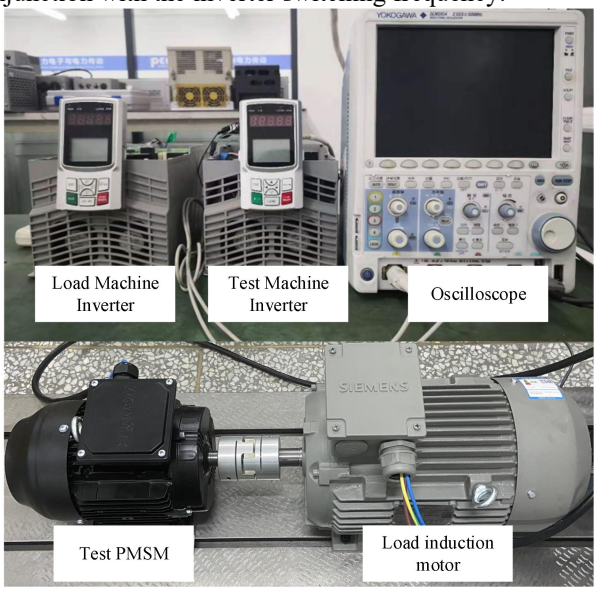

Fig. 6. Experimental platform.

C. Experimental Results and Analysis

The experimental results of initial magnet polarity identification with n = 100r/min is depicted in Fig. 6. Firstly, the initial position is observed through HF signal injection based method, and then the initial magnet polarity identification is completed by applying ZVV pulse at t = 40ms. The stator current amplitude stimulated by ZVV pulse is about 0.5A in the experiment, which cannot affect the normal operation of PMSM. In (a) and (b), the initial magnet polarity identification results are magnetic N pole and magnetic South (S) pole respectively. Finally, the accurate initial position can be obtained after the initial magnet polarity identification.

V. CONCLUSIONS

A novel initial magnet polarity identification method for PMSM drives is presented in this paper. Only a short ZVV pulse is applied and the current vector is excited, and then the initial magnet polarity is identified according to the relationship between the excited current vector and the initial position observed by HF signal injection based method. Simulation and experimental results show that the proposed method can realize the initial magnet polarity identification accurately and reliably.

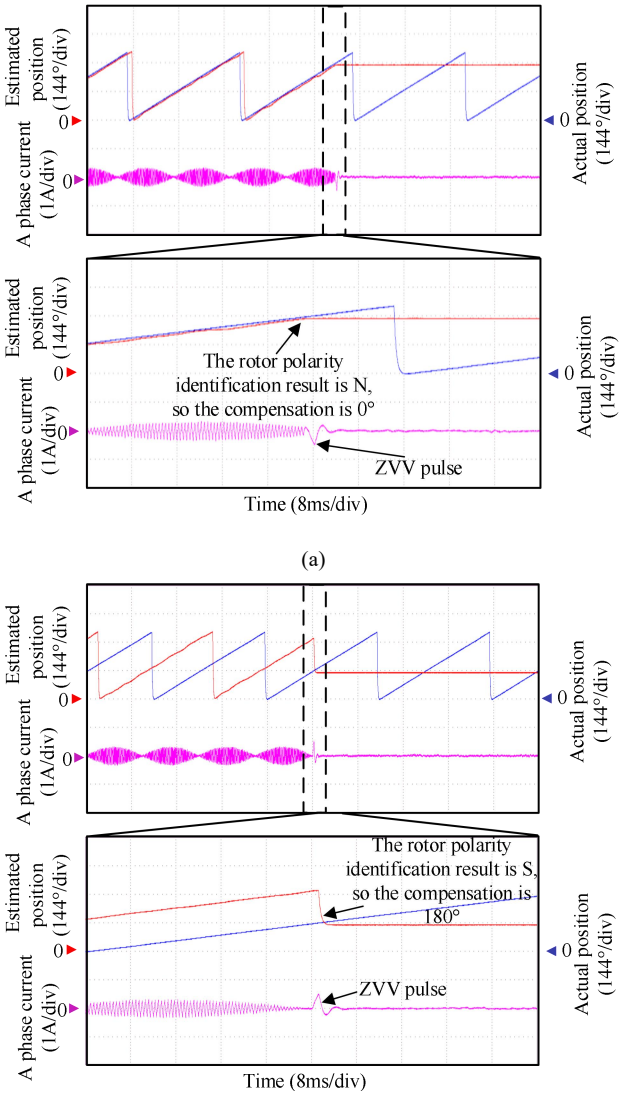

Fig. 7. Experimental result of initial magnet polarity identification based on ZVV method. (a): identification result is magnetic N pole; (b): identification result is magnetic S pole.

REFERENCES

[1] Q. Wang, S. Liu, G. Zhang, D. Ding, B. Li, G. Wang, and D. Xu, "Zero-Sequence Voltage Error Elimination Based Offline VSI Nonlinearity Identification for PMSM Drives," *IEEE Trans. Transp. Electrif.*, pp. 1-1, 2023.

[2] G. Zhang, R. Xiang, G. Wang, C. Li, G. Bi, N. Zhao, and D. Xu, “Hybrid Pseudorandom Signal Injection for Position Sensorless SynRM Drives With Acoustic Noise Reduction,” *IEEE Trans. Transp. Electrif.,* vol. 8, no. 1, pp. 1313-1325, 2022.

[3] G. Wang, R. Yang, and D. Xu, “DSP-Based Control of Sensorless IPMSM Drives for Wide-Speed-Range Operation,” *IEEE Trans. Ind. Electron.,* vol. 60, no. 2, pp. 720-727, 2013.

[4] S. Taniguchi, S. Mochiduki, T. Yamakawa, S. Wakao, K. Kondo, and T. Yoneyama, “Starting Procedure of Rotational Sensorless PMSM in the Rotating Condition,” *IEEE Trans. Ind. Appl.,* vol. 45, no. 1, pp. 194-202, 2009.

[5] K.-M. Choo, and C.-Y. Won, “Flying Start of Permanent-Magnet-Synchronous-Machine Drives Based on a Variable Virtual Resistance,” *IEEE Trans. Ind. Electron.,* vol. 68, no. 10, pp. 9218-9228, 2021.

[6] C. Li, G. Wang, G. Zhang, N. Zhao, and D. Xu, “Adaptive Pseudorandom High-Frequency Square-Wave Voltage Injection Based Sensorless Control for SynRM Drives,” *IEEE Trans. Power Electron.,* vol. 36, no. 3, pp. 3200-3210, 2021.

[7] Y. Li, G. Wang, W. Shen, G. Zhang, N. Zhao, X. He, and D. Xu, "High-Frequency Signal Injection using Extend State Observer for Position Sensorless PMSM Drives," in *ICIEA*, Kristiansand, Norway, 2020.

[8] P. L. Xu, and Z. Q. Zhu, “Novel Square-Wave Signal Injection Method Using Zero-Sequence Voltage for Sensorless Control of PMSM Drives,” *IEEE Trans. Ind. Electron.,* vol. 63, no. 12, pp. 7444-7454, 2016.

[9] Y. Wang, N. Guo, J. Zhu, N. Duan, S. Wang, Y. Guo, W. Xu, and Y. Li, “Initial Rotor Position and Magnetic Polarity Identification of PM Synchronous Machine Based on Nonlinear Machine Model and Finite Element Analysis,” *IEEE Trans. Magn.,* vol. 46, no. 6, pp. 2016-2019, 2010.